Article

Role of Asp102 in the Catalytic Relay System of Serine Proteases: A Theoretical Study

Toyokazu Ishida, and Shigeki Kato

J. Am. Chem. Soc., **2004**, 126 (22), 7111-7118• DOI: 10.1021/ja030405u • Publication Date (Web): 15 May 2004

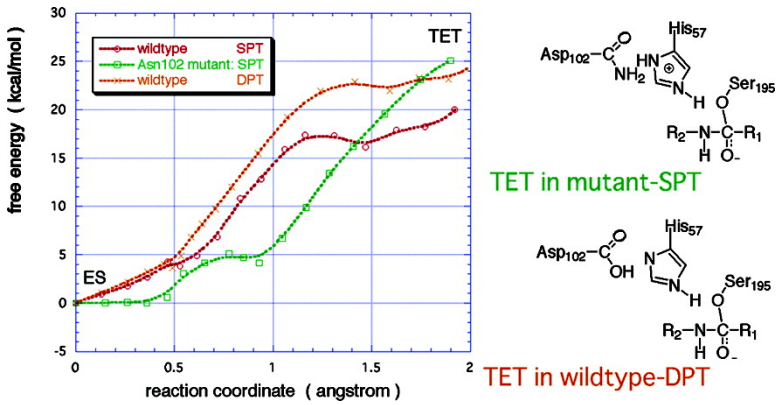

More About This Article

Additional resources and features associated with this article are available within the HTML version:

- Supporting Information
- Links to the 5 articles that cite this article, as of the time of this article download
- Access to high resolution figures
- Links to articles and content related to this article
- Copyright permission to reproduce figures and/or text from this article

View the Full Text HTML

J|A|C|S
ARTICLES
Published on Web 05/15/2004

Role of Asp102 in the Catalytic Relay System of Serine Proteases: A Theoretical Study

Toyokazu Ishida† and Shigeki Kato*

Contribution from the Department of Chemistry, Graduate School of Science, Kyoto University, Kitashirakawa, Sakyo-ku, Kyoto 606-8502, Japan

Received July 7, 2003; Revised Manuscript Received February 25, 2004; E-mail: shigeki@kuchem.kyoto-u.ac.jp

Abstract: The role of Asp102 in the catalytic relay system of serine proteases is studied theoretically by calculating the free energy profiles of the single proton-transfer reaction by the Asn102 mutant trypsin and the concerted double proton-transfer reaction (so-called the *charge-relay mechanism*) of the wild-type trypsin. For each reaction, the reaction free energy profile of the rate-determining step (the tetrahedral intermediate formation step) is calculated by using ab initio QM/MM electronic structure calculations combined with molecular dynamics−free energy perturbation method. In the mutant reaction, the free energy monotonically increases along the reaction path. The rate-determining step of the mutant reaction is the formation of tetrahedral intermediate complex, not the base (His57) abstraction of the proton from Ser195. In contrast to the single proton-transfer reaction of the wild-type, MD simulations of the enzyme−substrate complex show that the catalytically favorable alignment of the relay system (the hydrogen bonding network between the mutant triad, His57, Asn102, and Ser195) is rarely observed even in the presence of a substrate at the active site. In the double proton-transfer reaction, the energy barrier is observed at the proton abstraction step, which corresponds to the rate-determining step of the single proton-transfer reaction of the wild-type. Although both reaction profiles show an increase of the activation barrier by several kcals/mol, these increases have different energetic origins: a large energetic loss of the electrostatic stabilization between His57 and Asn102 in the mutant reaction, while the lack of stabilization by the protein environment in the double proton-transfer reaction. Comparing the present results with the single proton transfer of the wild-type, Asp102 is proven to play two important roles in the catalytic process. One is to stabilize the protonated His57, or ionic intermediate, formed during the acylation, and the other is to fix the configuration around the active site, which is favorable to promote the catalytic process. These two factors are closely related to each other and are indispensable for the efficient catalysis. Also the present calculations suggest the importance of the remote site interaction between His57 and Val213−Ser214 at the catalytic transition state.

1. Introduction

The His-Asp-Ser catalytic motif, so-called the *catalytic triad*, is totally conserved throughout the serine proteases family and believed to be responsible for the efficient catalysis. Although the catalytic roles of His57 and Ser195 are widely recognized, that of Asp102 still remains elusive. Especially, whether the proton in the His57-Asp102 hydrogen bond resides on His57 or Asp102, or how many protons are transferred in the catalytic pathway, has been a contentious issue.[1−3]

At the first discovery of the catalytic triad from the X-ray crystal structure of chymotrypsin, Blow and co-workers proposed that the triad motif renders Ser195 nucleophilicity through the electronic resonance structures.[4] Subsequent studies refined this mechanism by proposing an actual concerted double proton transfer (DPT) in the triad.[5] Because this DPT (so-called the *charge relay*) mechanism predicted that the pK_a of His57 was lower than that of Asp102, many experiments have been carried out to validate the basicity of His57. ^{1}H and ^{15}N NMR experiments showed that Asp102 does not change its protonic state during the reaction.[6,7] The neutron diffraction study with the monoisopropyl phosphate modified trypsin revealed that the proton is located on His57 at neutral pH conditions.[8] Based on those experimental facts, the single proton-transfer (SPT) mechanism where His57 is stabilized by the electrostatic effect of Asp102 is generally accepted at present. However, proton inventory measurements seem to favor the DPT in the specific cases.[9,10] These experiments revealed that DPT motion is apparently observed for oligopeptides which resemble naturally occurred

† Present address: Research Institute for Computational Science, National Institute of Advanced Industrial Science and Technology, Tsukuba Central 2,1-1-1; E-mail: toyokazu.ishida@aist.go.jp.

(1) Fersht, A. *Structure and Mechanism in Protein Science. A Guide to Enzyme Catalysis and Protein Folding*, 2nd ed.; W. H. Freeman and Company: New York, 1999.
(2) Wharton, C. W. In *Comprehensive Biological Catalysis*; Sinnott, M., Garner, C. D., First, E., Davies, G., Eds.; Accademic Press: 1998; Vol. 1, Chapter 9.
(3) Hedstrom, L. *Chem. Rev.* **2002**, *102*, 4501−4523.
(4) Blow, D. M.; Birktoft, J. J.; Hartley, B. S. *Nature* **1969**, *221*, 337−340.
(5) Hunkapiller, M. W.; Smallcombe, S. H.; Whitaker, D. R.; Richards, J. H. *Biochemistry* **1973**, *23*, 4723−4743.
(6) (a) Robillard, G.; Shulman, R. G. *J. Mol. Biol.* **1974**, *86*, 519−540. (b) Robillard, G.; Shulman, R. G. *J. Mol. Biol.* **1974**, *86*, 541−558.
(7) (a) Bachovchin, W. W.; Roberts, J. D. *J. Am. Chem. Soc.* **1978**, *100*, 8041−8047. (b) Bachovchin, W. W. *Proc. Natl. Acad. Sci. U.S.A.* **1985**, *82*, 7948−7951.
(8) (a) Kossiakoff, A. A.; Spencer, S. A. *Nature* **1980**, *288*, 414−416. (b) Kossiakoff, A. A.; Spencer, S. A. *Biochemistry* **1981**, *20*, 6462−6474.

substrates, although a single proton is transferred in the case of small substrates. To explore the catalytic role of Asp102, Craik and co-workers employed the site-directed mutagenesis technique.[11,12] Based on the kinetic and structural studies with the Asn102 mutant trypsin, they proposed that Asp102 is crucial to stabilize an appropriate His57 tautomer, which is favorable to abstract the proton from Ser195. Recently, the low-barrier hydrogen bond (LBHB) hypothesis has attracted much attention.[13−15] This proposes that a short, strong hydrogen bond formed between His57 and Asp102 could render His57 to be a more effective general base.

Despite those activities of experimental studies on serine protease reactions, theoretical studies based on ab initio calculations are still limited.[16−21] Most of earlier quantum mechanical calculations supported the DPT mechanism.[16] In these calculations, the catalytic triad was represented by an appropriate chemical species assuming the coordinates to be the same as the X-ray structures. Warshel and co-workers discussed the reaction mechanism of Asn102 mutant trypsin and the DPT mechanism based on the simple EVB/FEP calculations.[17,18] Although their calculations could reproduce the experimental trend, no theoretical interpretation has emerged for the complete picture of the reaction mechanism at present.

In the previous paper,[21] we studied the acylation process of serine proteases by ab initio QM/MM calculations combined with molecular dynamics−free energy perturbation (MD−FEP) simulations and revealed that the rate-determining step is the tetrahedral intermediate (TET) formation process. It was also shown that the electrostatic interaction with the protein environment plays a critical role for the effective catalytic activity. In the present work, we focus on the role of Asp102 in the catalytic relay system. For this purpose, we calculated the free energy profiles for the SPT of Asn102 mutant trypsin and the DPT of wild-type by ab initio QM/MM, MD−FEP method. We only dealt with the TET formation process because this can be regarded as the rate-determining step as in the SPT of wild-type.

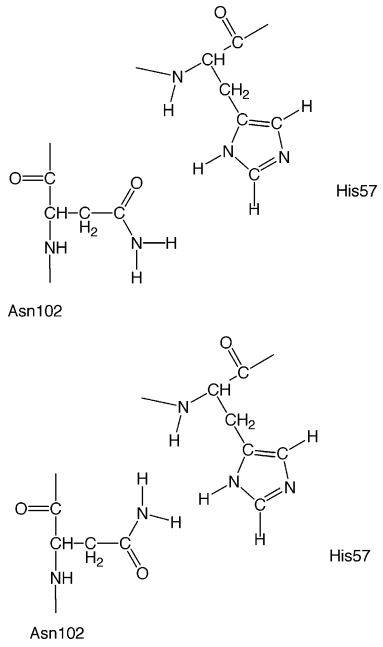

Figure 1. Two chemically distinct conformations of the Asn102 mutant trypsin. (Above) The conformation where the side chain NH_2 group is oriented toward the active site cleft. The O_δ atom of Asn102 could accept the hydrogen bonds from the His57 residue. (Below) The conformation where the side chain amide group is rotated by ∼180° around the $C_\beta-C_\gamma$ bond.

2. Computational Details

2.1. Ab Initio QM/MM, MD−FEP Calculations. We used the same method as in the previous work for calculating the free energy profile.[21]

The total free energy was calculated along the minimum energy reaction path determined by the restrained QM/MM optimizations as follows:

$$F \simeq G_{QM}(\boldsymbol{R}_{QM}^{min}) - k_B T \ln \int \exp\{-\beta[E^{QM/MM}(\boldsymbol{R}_{QM}^{min},\boldsymbol{R}^{MM}) + E^{MM}(\boldsymbol{R}^{MM})]\}\, d\boldsymbol{R}_{MM} \quad (1)$$

The first term represents the vibrational free energy in the QM region evaluated by ab initio QM/MM calculations based on the harmonic approximation. In the present case, $E_{QM/MM}$ was given by

$$E_{QM/MM} = E_{QM/MM}^{elec} + E_{QM/MM}^{vdw} + E_{QM/MM}^{strain} \quad (2)$$

where the standard AMBER (parm.96) force field[22] was employed to describe the MM region. The second term of eq 1 represents the free energy contribution from MM region, which is calculated by the MD−FEP technique[23] along the minimum energy path.

2.2. Free Energy Profile of Asn102 Mutant Trypsin. The overall strategy to calculate the free energy profile was the same as that in previous work. At first, a suitable reaction coordinate $\mathbf{R}_c$, which is adequate to describe the chemical reaction, was selected. The reaction coordinate $\mathbf{R}_c$ was defined as a function of some geometric parameters: $\mathbf{R}_c = W(q_1, q_2, ..., q_n)$, where q_i is an appropriate bond length or

(9) (a) Elrod, J. P.; Hogg, J. H.; Quinn, D. M.; Venkatasubban, K. S.; Schowen, R. L. *J. Am. Chem. Soc.* **1980**, *102*, 3917−3922. (b) Quinn, D. M.; Elrod, J. P.; Ardis, R.; Friesen, P.; Schowen, R. L. *J. Am. Chem. Soc.* **1980**, *102*, 5358−5365. (c) Stein, R. L.; Elrod, J. P.; Schowen, R. L. *J. Am. Chem. Soc.* **1983**, *105*, 2446−2452.
(10) Stein, R. L. *J. Am. Chem. Soc.* **1983**, *105*, 5, 5111−5116.
(11) Craik, C. S.; Roczniak, S.; Largman, C.; Rutter, W. J. *Science* **1987**, *237*, 909−913.
(12) Sprang, S.; Standing, T.; Fletterick, R. J.; Stroud, R. M.; Finer-Moore, J.; Xuong, N.-H.; Hamlin, R.; Rutter, W. J.; Craik, C. S. *Science* **1987**, *237*, 905−909.
(13) (a) Frey, P. A.; Whitt, S. A.; Tobin, J. B. *Science* **1994**, *264*, 1927−1930. (b) Cleland, W. W.; Frey, P. A.; Gerlt, J. A. *J. Biol. Chem.* **1998**, *273*, 25529−25532.
(14) (a) Perrin, C. L.; Nielson, J. B. *Annu. Rev. Phys. Chem.* **1997**, *48*, 511−544. (b) Mildvan, A. S.; Harris, T. K.; Abeygunawardana, C. *Methods Enzymol.* **1999**, *308*, 219−245.
(15) (a) Cassidy, C. S.; Lin, J.; Fery, P. A. *Biochemistry* **1997**, *36*, 4576−4584. (b) Lin, J.; Cassidy, C. S.; Fery, P. A. *Biochemistry* **1998**, *37*, 11940−11948. (c) Lin, J.; Westler, W. M.; Clealand, W, W.; Markley, J. L.; Fery, P. A. *Proc. Natl. Acad. Sci. U.S.A.* **1998**, *95*, 14664−14668. (d) Neidhart, D.; Wei, Y.; Cassidy, C. S.; Lin, J.; Cassidy, C. S.; Clealand, W, W.; Fery, P. A. *Biochemistry* **2001**, *40*, 2439−2447. (e) Westler, W. M.; Fery, P. A.; Lin, J.; Wemmer, D. E.; Morimot, H.; Williams, P. G.; Markley, J. L. *J. Am. Chem. Soc.* **2002**, *124*, 4196−4197.
(16) (a) Umeyama, H.; Imamura, A.; Nagato, C.; Hanano, M. *J. Theor. Biol.* **1973**, *41*, 485−502. (b) Scheiner, S.; Kleier, D. A.; Lipscomb, W. N. *Proc. Natl. Acad. Sci. U.S.A.* **1975**, *72*, 2606−2610. (c) Dewar, M. J. S.; Storch, D. M. *Proc. Natl. Acad. Sci. U.S.A.* **1985**, *82*, 2225−2229.
(17) (a) Warshel, A.; Russell, S. *J. Am. Chem. Soc.* **1986**, *108*, 6569−6579. (b) Warshel, A.; Naray-Szabo, G.; Sussman, F.; Hwang, J. K. *Biochemistry* **1989**, *28*, 3629−3637.
(18) Warshel, A. *Computer Modeling of Chemical Reactions in Enzymes and Solutions*; John Wiely & Sons: New York, 1991.
(19) (a) Schröder, S.; Daggett, V.; Kollman, P. *J. Am. Chem. Soc.* **1991**, *113*, 8922−8925. (b) Daggett, V.; Schröder, S.; Kollman, P. *J. Am. Chem. Soc.* **1991**, *113*, 8926−8935.
(20) (a) Stanton, R. V.; Peräkylä, M.; Bakowies, D.; Kollman, P. A. *J. Am. Chem. Soc.* **1998**, *120*, 3448−3457. (b) Peräkylä, M.; Kollman, P. A. *J. Am. Chem. Soc.* **2000**, *122*, 3436−3444.
(21) Ishida, T.; Kato, S. *J. Am. Chem. Soc.* **2003**, *125*, 12035−12048.
(22) (a) Cornell, W. D.; Cieplak, P.; Bayly, C. I.; Gould, I. R.; Merz, K. M., Jr.; Ferguson, D. M.; Spellmeyer, D. C.; Fox, T.; Caldwell, J. W.; Kollman, P. A. *J. Am. Chem. Soc.* **1995**, *117*, 5179−5197. (b) Kollman, P.; Dixon, R.; Cornell, W.; Fox, T.; Chipot, C.; Pohorille, A. In *Computer Simulation of Biomolecular Systems, Vol. 3*; van Gunsteren, W. F., Weiner, P. K., Wilkinson, A. J., Eds.; Kluwer Academic Publishers: 1997.
(23) Kollman, P. *Chem. Rev.* **1993**, *93*, 2395−2417.

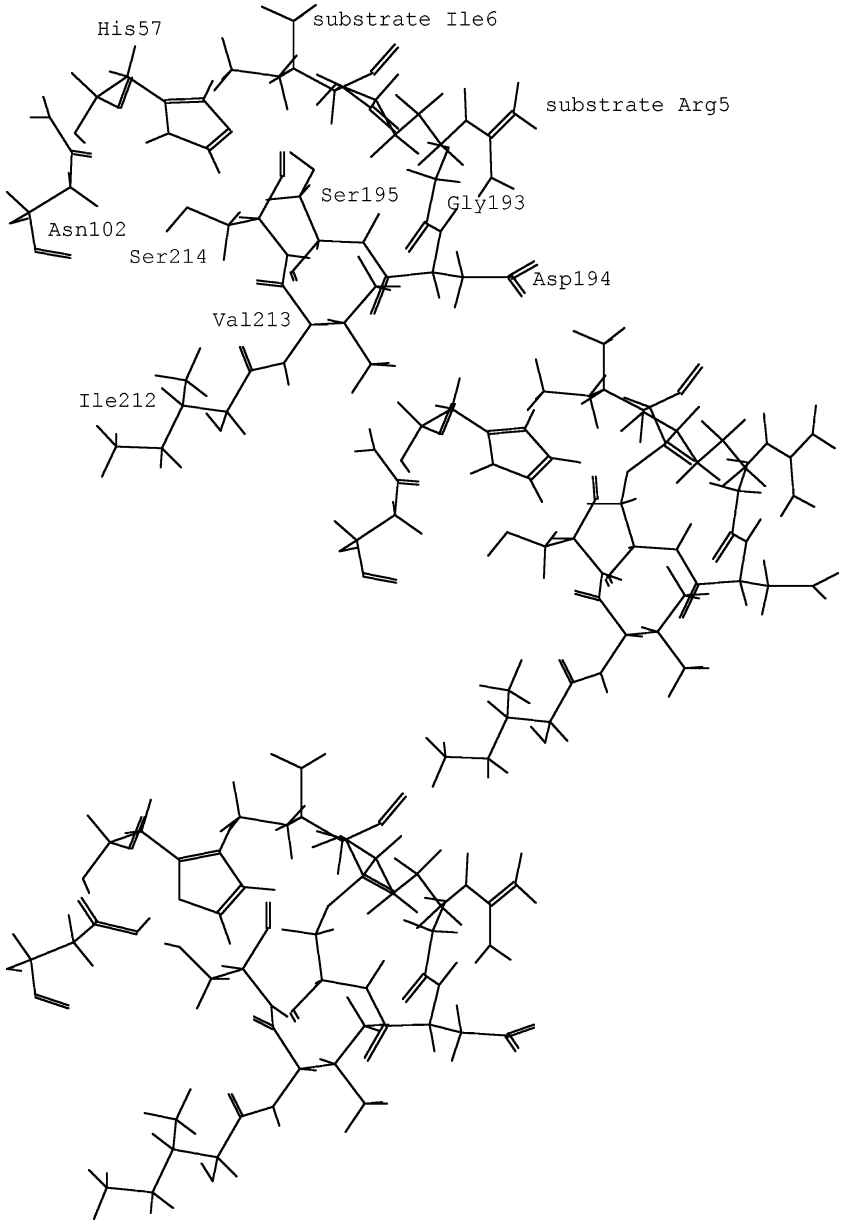

Figure 2. Optimized structures of the ES/TET state of the Asn102 mutant and the TET state of the double proton-transfer reaction of the wild-type (ab initio QM/MM HF/6-31(+)G*(*)/AMBER level). (Top) ES state of the Asn102 mutant. (Middle) TET state of the Asn102 mutant. (Bottom) TET state of the double proton-transfer reaction. Only selected amino residues around the active site are shown in this figure.

angle, etc.. Then the minimum energy reaction path was determined by the restrained QM/MM optimizations by fixing the selected reaction coordinate. In the case of Asn102 mutant reaction, q_1 is the bond length of O_γ-H_γ in Ser195, and q_2 is the bond distance between O_γ of Ser195 and the carbonyl carbon of the scissile peptide. For the DPT reaction, two of q_i are the same as those in the mutant reaction, and q_3 is the $N_\delta-H_\delta$ bond length in His57. Because the molecular system for the DPT reaction is the same as the earlier wild-type/SPT calculations, we only give a description of the calculation procedure for the Asn102 mutant.

The initial geometry of the Asn102 mutant complex was the same as that of the wild-type (trypsin complex with an inhibitor from Bitter Gourd determined to 1.6 Å resolution, PDB code 1MCT). The Asn102 was placed at the original Asp102 position: we adopted the conformation where the side chain N_δ atom of Asn102 was oriented toward outside the main chain amide groups of Ala56 and His57 (Figure 1). The sequence of the substrate was the same as that in the previous study. (Cys3-Pro4-Arg5-Ile6-Trp7-Met8, the serial number comes from the original inhibitor sequence) and placed at the same position at the active site. All crystal waters used were retained at the same positions. Nine chloride ions were added at the positions of largest electrostatic potentials to neutralize the total charge.

The QM region was the same as that in the wild-type calculations except for the side chain of Asn102. The boundaries between QM and MM regions were saturated by link hydrogen atoms: $C_\alpha-C_\beta$ bond of His57 and Asn102; $C_\alpha-NH$, $C_\alpha-CO$ bonds of Ser195; $C_\alpha-C_\beta$, $C_\alpha-NH$ bonds of substrate Arg5; and $C_\alpha-C_\beta$, $C_\alpha-CO$ bonds of substrate Ile6. In all ab initio QM/MM geometry optimizations, we employed the HF method with the same basis set as that in the previous study, 6-31(+)G*(*)[24] (diffuse functions were added to O_γ of Ser195 and the scissile peptide portion of the substrate, and p-functions were added to H_γ of Ser195 and H_δ of His57). The electron correlation energy at each HF optimized point was obtained by single-point MP2 calculation with cc-pVDZ basis set[25] augmented by diffuse functions on the same atoms described above, (aug)-cc-pVDZ.

(24) Hehre, W. J.; Radom, L.; van Schleyer, P. R.; Pople, J. A. *Ab Initio Molecular Orbital Theory*; John Wiely & Sons: New York, 1986.

Table 1. Selected Geometrical Parameters of ab Initio QM/MM Full-Geometry Optimized Structures[a] along the Minimum Energy Reaction Path (in Å)

	Ans102 mutant		double proton transfer		
	ES	TET	ES[b]	TS	TET
O_γ(Ser195)—H_γ(Ser195)	0.952	1.700	0.957	1.616	1.852
O_γ(Ser195)—N_ϵ(His57)	2.902	2.726	2.766	2.642	2.834
N_ϵ(His57)—H_γ(Ser195)	2.004	1.034	1.834	1.036	1.007
$O_{\delta1}$(Asp102)—N_δ(His57)			2.723	2.647	2.705
$O_{\delta1}$(Asp102)—H_δ(His57)			1.718	0.998	0.986
H_δ(His57)—N_δ(His57)			1.021	1. 655	1.726
O_δ(Asn102)—N_δ(His57)	2.834	2.817			
O_δ(Asn102)—H_δ(His57)	1.875	1.863			
H_δ(His57)—N_δ(His57)	1.003	1.010			
O_δ(Asn102)—N(His57)	2.930	2.894			
$O_{\delta2}$(Asp102)—N_δ(His57)			3.503	3.455	3.477
$O_{\delta2}$(Asp102)—H_δ(His57)			2.676	2.331	2.310
$O_{\delta2}$(Asp102)—N(His57)			2.731	2.742	2.747
O_γ(Ser195)—C(scissile bond)	2.715	1.564	2.672	1.915	1.493
N—C(scissile peptide bond)	1.360	1.486	1.392	1.447	1.520
C═O(in scissile bond)	1.211	1.276	1.203	1.229	1.284
O(scissile peptide)—N(Ser195)	3.690	2.990	3.841	3.331	3.128
O(scissile peptide)—HN(Ser195)	2.721	2.055	2.864	2.366	2.170
O(scissile peptide)—N(Gly193)	2.756	2.727	2.772	2.726	2.703
O(scissile peptide)—HN(Gly193)	1.742	1.709	1.768	1.710	1.683
O_γ(Ser214)—$O_{\delta1}$(Asp102)			2.530	2.586	2.595
H_γ(Ser214)—$O_{\delta1}$(Asp102)			1.527	1.604	1.616
O(carbonyl,Ser214)—C_ϵ(His57)	3.057	2.903	2.972	2.879	2.875
O(carbonyl,Val213)—C_ϵ(His57)	4.586	4.162	4.292	3.591	3.576

[a] All geometry optimizations were performed at the QM/MM HF/6-31(+)G*(*) level. [b] These values are adopted from ref 21.

In the MD−FEP calculations, the solvated protein system was defined by adding a sphere of TIP3P[26] water molecules with a 30 Å radius centered on the O_γ site of Ser195: the solvated structure consisted of 128 crystal waters and additional 3618 water molecules. We adopted the Nosé−Hoover-chain/r-RESPA[27−29] algorithm to generate the NVT ensemble with the temperature of 310 K. The free energy differences were calculated by the double-wide sampling method.[30] A total of 16 windows were used in MD−FEP calculations (18 windows for DPT reaction). In each window, the simulation consisted of a 10 ps equilibration process and 30 ps averaging run. The relative free energies were calculated as the average of the forward/backward simulation results.

3. Results and Discussion

3.1. ES Complex of Asn102 Mutant Trypsin. The optimized structure around the active site of ES complex is shown in Figure 2. The selected geometric parameters at ES are summarized in Table 1. Although the optimized ES geometry around the oxyanion hole is similar to that of wild-type in general, we can find a remarkable structural difference between the two systems. While O_δ of Asn102 is hydrogen bonded to N_δ and the main chain NH group of His57, N_δ of Asn102 is hydrogen bonded to the main chain carbonyl group of Asp100, not the hydroxyl group of Ser214 as in the wild-type.

A 1 ns MD simulation in aqueous phase was performed to further analyze conformational changes introduced by the mutational effect. The equilibrium values of bond lengths and angles (r_{eq}, θ_{eq}) in the QM region were fixed at the QM/MM optimized values in ES complex.

On the whole, the average structure around the oxyanion hole and the substrate binding site is similar to that of the wild-type ES complex. However, the rotational orientation of the imidazole ring of His57 varies largely: the average dihedral angle χ_2 of His57 is $\sim 150° \pm 70°$, while that of the wild-type is $\sim -90° \pm 10°$. Because of this flexibility of the imidazole ring, the catalytically favorable alignment of the mutant-relay system (hydrogen bonding between His57 and Asn102, between His57 and Ser195) is rarely observed during the simulation time.

3.2. Asn102 Mutant Reaction: From ES to TET. The minimum energy reaction path depicted on the 2D-reaction coordinate diagram is shown in Figure 3. For a comparison, the reaction path of the wild-type SPT is also included in this figure. Although the two reactive modes (the proton transfer from Ser195 to His57 and the nucleophilic attack of Ser195 to the scissile peptide) progress in a concerted manner in the wild-type, the proton transfer starts after a large orbital overlap is achieved between the hydroxyl group of Ser195 and the carbonyl group of the scissile peptide for the mutant reaction. This profile seems to be a stepwise path rather than a concerted one.

The free energy profile along the minimum energy path is shown in Figure 4. Although there was observed a shallow minimum on the *potential energy* surface at the QM/MM-HF level calculations, the *free energy* monotonically increases along the path. The change of the curvature of free energy observed at $\mathbf{R}_c \approx 0.9$ Å is attributed to the stepwise nature of the minimum energy path as mentioned above. Compared with the wild-type/SPT reaction whose free energy curve is also given in Figure 4, the ES-TET free energy difference is larger for the Asn102 mutant reaction by ~5 kcal/mol. This mainly comes from the QM contribution to the energy as seen in Table 2. As was mentioned in the previous paper,[21] TET is a local energy minimum on the potential energy surface, originated from a limited availability of the present QM/MM optimizations. For the reaction to proceed, TET must be converted into the structure (TET′) preferable to abstract the proton from His57. We regarded this TET′ structure as the real *tetrahedral intermediate* in the previous paper. This process is completely exothermic in the wild-type/SPT reaction. In the case of the Asn102 mutant, the reaction seems to proceed in a similar way, and the rate-determining step is considered to be the formation of TET. For the Asn102 mutant reaction, the transition state (TS) structure is considered to be very similar to that of the TET. To clarify the energetic relation of the reactions, the schematic free energy diagram is given in Figure 5. Note that the stabilization by solvation is larger for the mutant reaction than the wild-type reaction.

The selected geometric parameters of TET are included in Table 1. No apparent conformational change is observed between His57 and Asn102 along the reaction coordinate, although two hydrogen bonds between the carbonyl oxygen of the scissile bond and the main chain NH groups of Gly193 and Ser195 are formed in the oxyanion hole region at TET.

3.3. Double Proton-Transfer Reaction: From ES to TET. The minimum energy reaction path for the wild-type/DPT process determined in a 3D-coordinate space is projected onto each 2D-coordinate plane, and the results are depicted in Figure

(25) Kendall, R. A.; Dunning, T. H.; Harrison, R. J. *J. Chem. Phys.* **1992**, *96*, 6796−6806.
(26) Jorgensen, W. L.; Chandrasekhar, J.; Madura, J. D.; Impey, R. W.; Klein, M. L. *J. Chem. Phys.* **1983**, *79*, 926−935.
(27) Martyna, G. J.; Klein, M. L.; Tuckerman, M. *J. Chem. Phys.* **1992**, *97*, 2635−2643.
(28) Tuckerman, M.; Berne, B. J.; Martyna, G. J. *J. Chem. Phys.* **1992**, *97*, 1990−2001.
(29) Martyna, G. J.; Tuckerman, M. E.; Tobias, D. J.; Klein, M. L. *Mol. Phys.* **1996**, *87*, 1117−1157.
(30) Jorgensen, W. L.; Ravimohan, C. *J. Chem. Phys.* **1985**, *83*, 3050−3054.

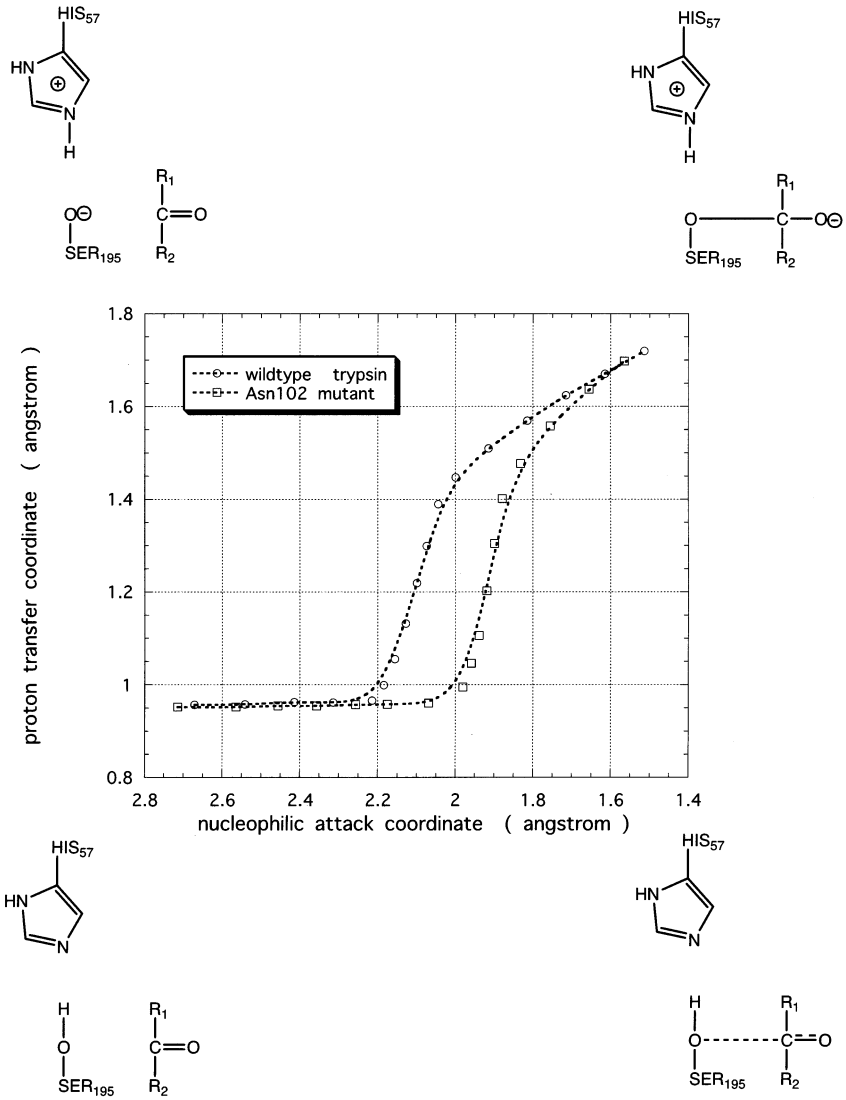

Figure 3. The minimum energy reaction path of the first step reaction (from ES to TET) depicted in the 2D reaction coordinate diagram. For a comparison, the SPT reaction path of the wild-type is included in this figure. The *x*-axis defines the nucleophilic attack coordinate (interatomic distance between O_γ of Ser195 and the carbonyl carbon of the scissile bond), and the *y*-axis is the proton-transfer coordinate (bond length of $O_\gamma-H_\gamma$ in Ser195). The four structures depicted on each square corner represent the asymptotic structures along each reaction direction.

6. The DPT motion begins only when the nucleophilic attack coordinate becomes ∼2.2 Å. These proton transfers do not proceed in a completely concerted manner: the proton between His57 and Asp102 moves prior to the base (His57) abstraction of the proton from Ser195.

The free energy profile is shown in Figure 4. The calculated barrier height is ∼22.9 kcal/mol, which is ∼5 kcal/mol higher than that of the wild-type SPT. We found two characteristic differences in the energy components between the two mechanisms. One is that the QM part of energy of TET is lower for DPT by ∼5 kcal/mol than that of SPT. The other is that the electrostatic stabilization by the interaction with the protein environment is smaller for the TET of DPT by ∼8 kcal/mol than that of SPT, because Asp102 and His57 are in neutral form and the negative charge is localized at the oxyanion of the scissile peptide in the TET of DPT. The solvation stabilization is also smaller for the TET of DPT by ∼3 kcal/mol than that of SPT. Thus the difference in the free energy between the TETs of two reaction mechanisms mainly comes from the electrostatic contribution of protein.

Note that these results are consistent with earlier semiempirical calculations that show the DPT being favored without the protein environment.[16,19]

3.4. Remote Site Interaction along the Reaction Path. The QM/MM nonbonded interaction energy was decomposed into each amino residue contribution to analyze the origin of interaction from a structural viewpoint. The analyses were based on the optimized structures along the minimum energy path. To clarify the energetic difference between wild-type/SPT reactions, the contribution from each amino residue was calculated by

$$\Delta\Delta E^{\mathrm{QM/MM}}_{i-\mathrm{residue}} = (\Delta E^{\mathrm{QM/MM}}_{i-\mathrm{residue}})_{\mathrm{mutant/DPT}} - (\Delta E^{\mathrm{QM/MM}}_{i-\mathrm{residue}})_{\mathrm{wild-type/SPT}}$$

where

$$\Delta E^{\mathrm{QM/MM}}_{i-\mathrm{residue}} = (E^{\mathrm{QM/MM}}_{i-\mathrm{residue}})_{\mathrm{TET}} - (E^{\mathrm{QM/MM}}_{i-\mathrm{residue}})_{\mathrm{ES}}$$

The energetic components of the wild-type/SPT reaction ($\Delta E^{\mathrm{QM/MM}}_{i-\mathrm{residue}}$) were adopted from the previous work.[21]

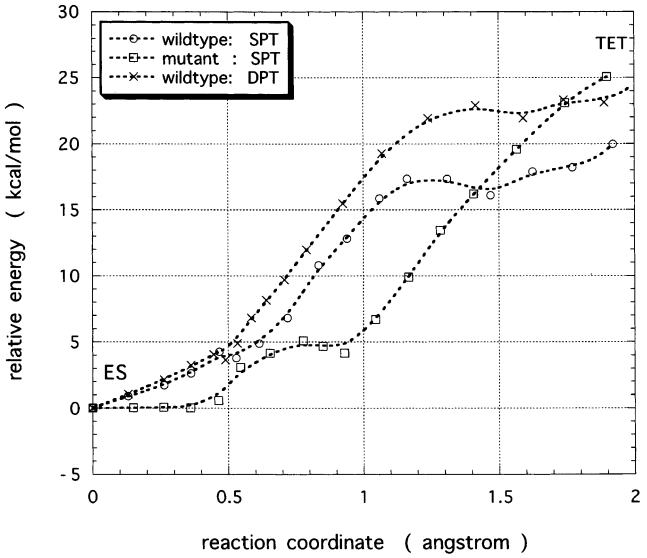

Figure 4. Comparison of the free energy profile between three different reactions. The wild-type/SPT result is adopted from the previous work.[21] In the DPT profile, the reaction coordinate is projected onto the related reaction path determined in the 2D coordinate plane.

Table 2. Free Energy Calculation Results (From ES to TET) in Each Reaction Profile (in kcal/mol)

	Ans102 mutant	wildtype	
	SPT	DPT	SPT[c]
QM part contribution[a]	53.65	33.85	39.18
(E(QM) part)	(69.87)	(43.83)	(52.43)
(E_{MP2})	(−18.04)	(−11.14)	(−14.70)
(ZPE)	(−0.14)	(−0.07)	(−0.13)
($T\Delta S$)	(−1.96)	(−1.25)	(−1.58)
protein contribution[b]	−16.07 ± 1.94	−3.37 ± 0.49	−11.79 ± 0.92
solvent contribution[b]	−12.51 ± 0.14	−3.65 ± 0.15	−7.02 ± 0.01
total free energy[b]	25.07 ± 2.08	26.83 ± 0.64	20.37 ± 0.93

[a] QM part contribution includes the zero-point energy and entropy contributions in 310 K. MP2 electron correlation energies were calculated at the MP2/(aug)-cc-pVDZ//HF/6-31(+)G*(*) level. ZPE and entropy contributions were calculated by a numerical differentiation method at the HF/6-31(+)G*(*) level. [b] The error estimates indicate the difference between forward and backward MD−FEP simulation runs. [c] These values are adopted from ref 21.

Figure 7 (above/below) shows the decomposition results in the mutant/DPT reaction, respectively. Two notable points are observed in the mutant reaction. Because of a structural change between Asn102 and Ser214, Ser214 has some favorable contribution to the total interaction energy. The substrate Pro4, which is located above the imidazole ring of His57, has a large favorable interaction with the active site. In the case of the DPT mechanism, unfavorable energy contributions originate from the residues that have a strong interaction with Asp102 in the wild-type: His57 and Val213−Ser214. In particular, Ser214 shows a large unfavorable contribution to the total interaction. The reason is mainly due to a loss of the electrostatic stabilization by the neutral Asp102.

From the analyses of two different types of reactions, it has been observed that only a limited region of protein environment is responsible for the efficient catalysis. The interaction around the oxyanion hole shows similar behavior in each reaction, while that of Ser214 is distinctly different. According to the conventional notation by Schechter and Berger,[31] the binding sites between proteases and polypeptide substrates are categorized in terms of the P_n-S_n interactions.[1−3] In the present calculations,

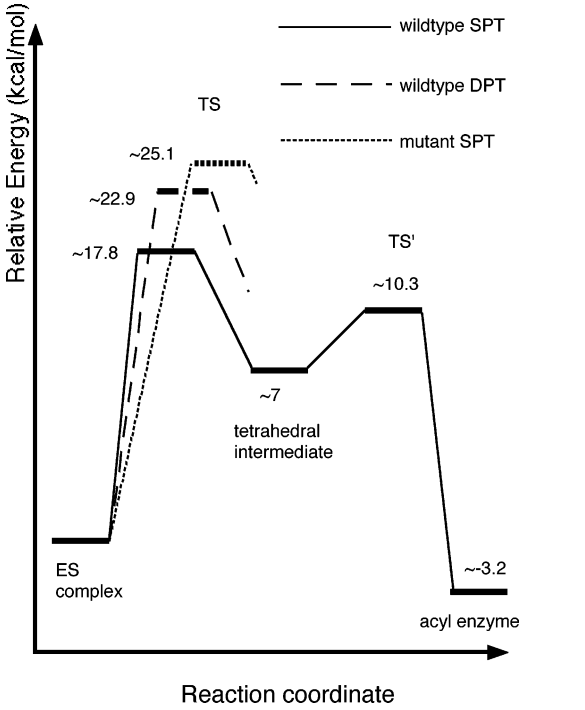

Figure 5. Schematic free energy diagram along the reaction coordinate among the three types of reactions. The acylation profile of the wild-type/SPT reaction is adopted from the previous work.[21] Note that, for the mutant SPT/wild-type DPT reaction, we only considered the free energy profile of the rate-determining step (tetrahedral intermediate formation process).

there are few configurational differences in the primary binding site S_1 between the two types of reactions. Apparent structural differences are observed at the S_2 site, a hydrophobic groove surrounded by His57, Leu99, Ser214, and Trp215.

3.5. Role of Asp102 in the Catalytic Relay System. From the present results of the Asn102 mutant reaction, Asp102 seems to play two important roles in the catalytic process. One is to stabilize the positive charge developed in the adjacent His57 by the strong electrostatic effect, and the other is to fix the alignment of the catalytic residues around the active site. As seen in Figures 3 and 4, Asn102 largely reduces the ability of His57 to abstract the proton from Ser195, i.e., basicity, compared to the Asp102 case.

In the MD simulation of the Asn102 mutant ES complex, there is less opportunity to find the catalytically favorable alignment of the mutant-triad residue. This is mainly attributed to the ring flipped conformation of His57 ($\chi_2 \approx 150°$), where the effective hydrogen bond between His57 and Ser195 is almost broken. To achieve the catalytic conformation where His57 is hydrogen bonded to Ser195, an additional energy penalty to flip the imidazole ring of His57 by ∼140° is needed. We estimated this additional energy by calculating the potential of mean force (pmf). The free energy $F(\chi_2)$ as the function of the dihedral angle χ_2 is related to the relative probability density $\rho(\chi_2)$ by

$$F(\chi_2) = -k_B T \ln\rho(\chi_2) + C$$

The result is shown in Figure 8, where we can see that the catalytic conformation is thermodynamically less stable by ∼1.3

(31) Schechter, I.; Berger, A. *Biochem. Biophys. Res. Commun.* **1967**, *27*, 157−162.

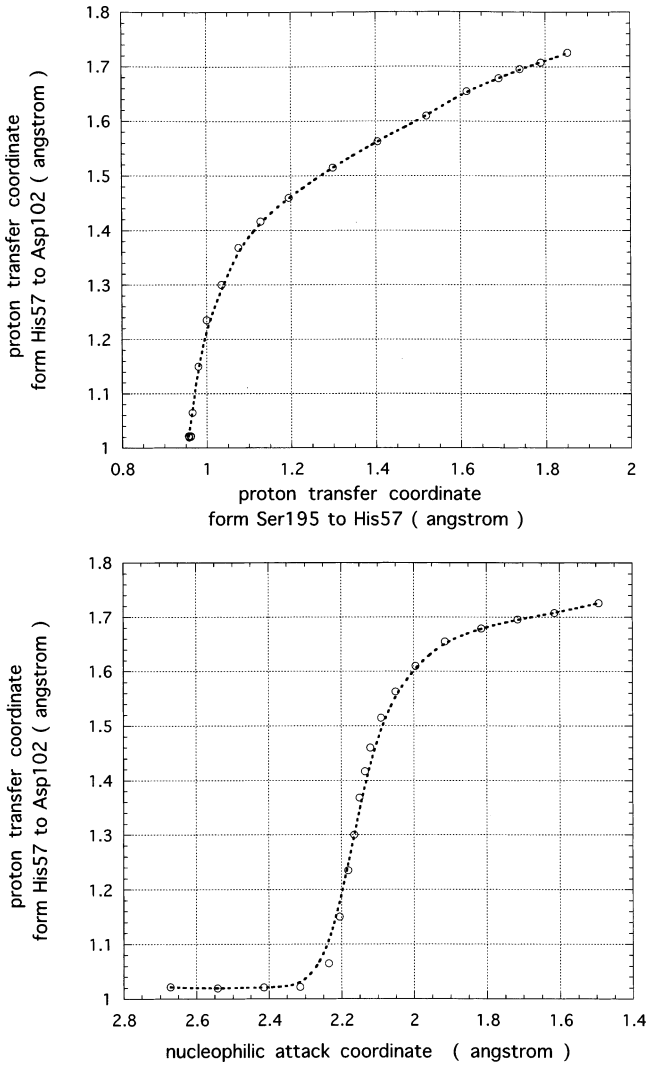

Figure 6. Minimum energy reaction path of the first step reaction (from ES to TET) of the DPT reaction projected onto the 2D reaction coordinate diagram. (Above) The *x*-axis defines one proton-transfer coordinate (bond length of $O_\gamma-H_\gamma$ in Ser195), and the *y*-axis is the other proton-transfer coordinate (bond length of $H_\delta-N_\delta$ in His57). (Below) The *x*-axis defines the nucleophilic attack coordinate (interatomic distance between O_γ of Ser195 and the carbonyl carbon of the scissile bond), and the *y*-axis is one proton-transfer coordinate (bond length of H_δ-N_δ in His57).

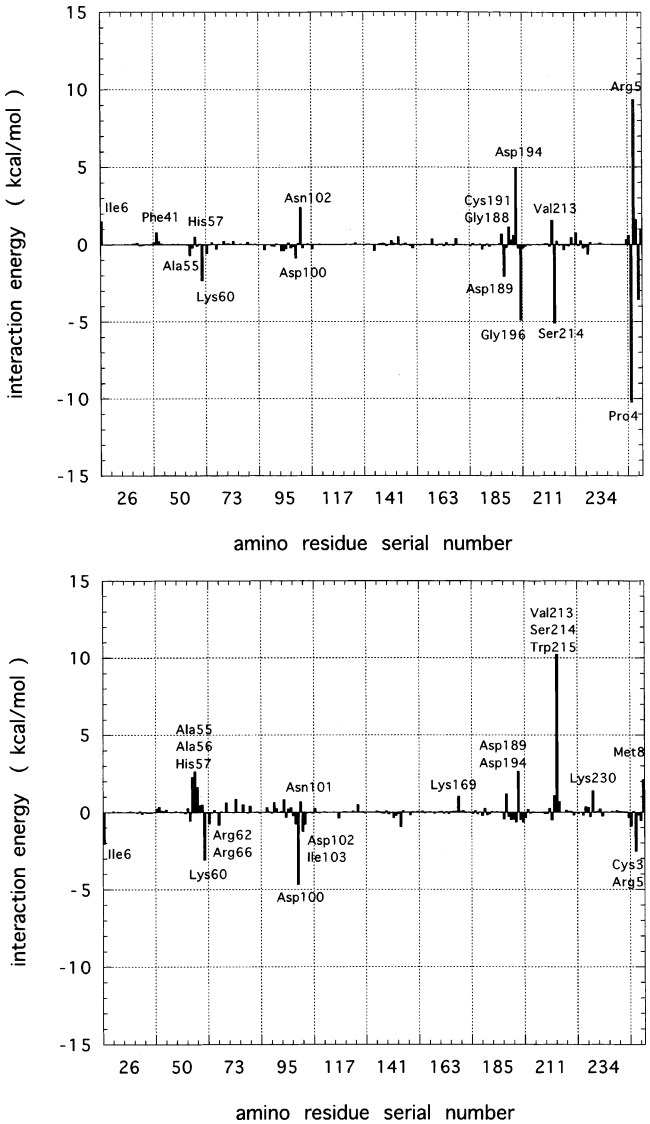

Figure 7. Interaction energy decomposition between QM (active site) and MM (the rest of protein environment) regions: (above) decomposition of the Asn102 mutant reaction and (below) decomposition of the double proton-transfer reaction. All contributions of crystal waters and counterions were omitted. Each energy component shows the difference of the energy difference from the wild-type SPT reaction. See details in the text.

kcal/mol than the anti-catalytic one. This result is consistent with the X-ray crystal structure of Asn102 mutant trypsin where two configurations of His57 are observed and the rotated conformation toward the solvent side is a major structure.[12] From Figure 8, the barrier height to flip the imidazole ring of His57 is estimated to be ∼2.2 kcal/mol.

Based on the X-ray crystal structure of Asn102 mutant trypsin where the imidazole ring of His57 was displaced from the active site toward the solvent side, Craik and co-workers concluded that the reduced activity of the mutant is mainly due to an unfavorable tautomeric state of His57, which is unable to accept the hydroxyl proton from Ser195.[11,12] Though this conformational change may be one of the anti-catalytic factors, it is hard to explain that the magnitude of decrease in k_{cat} by $\sim 10^4$ comes only from the conformational effect. The present results show that the main anti-catalytic factor is the loss of the strong electrostatic stabilization between His57 and Asn102 in the TET structure as discussed in section 3.2. If we assume that the overall reaction rate is dominated by the formation of TET as observed in the wild-type reaction, the present results agree reasonably well with the experimental findings.

In the case of the DPT mechanism, the calculated QM region energy shows that the protonated Asp102 is more stable than the ionized one even in the active site of the enzyme. The anti-catalytic effect that prevents the DPT motion is a loss of the electrostatic stabilization between the active site and the surrounding protein. Especially, the electrostatic interaction between two domains, His57 and Val213−Ser214, is a critical catalytic factor. This result implies that the protein environment around the active site is designed to stabilize the ionic intermediate state, Asp(−) His(+) oxyanion(−), formed along the catalytic pathway by the particular residues. Table 3 shows the averaged structural parameters at TET state of wild-type SPT/DPT reactions. The neutralized residues apparently loses the character that fixes the surrounding residues to stabilize TET structure. Though the averaged structures around the oxyanion

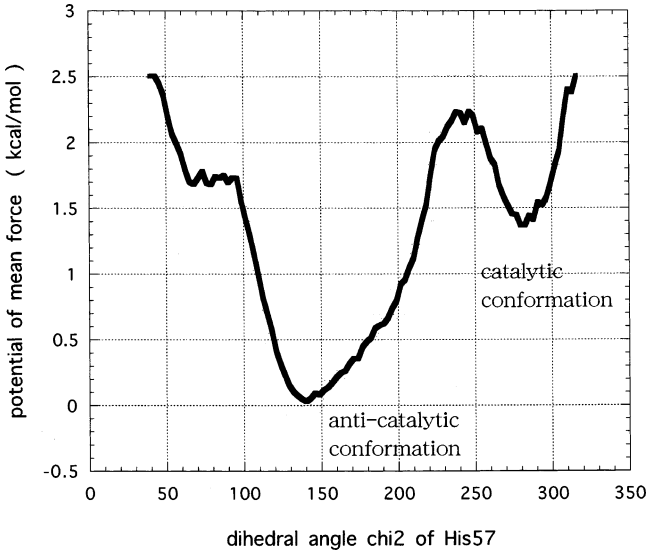

Figure 8. Potential of mean force as the function of dihedral angle χ_2 in His57. The catalytic conformation has a structure where His57 is hydrogen bonded to Ser195. See details in the text.

Table 3. Averaged Geometrical Parameters of Wild-Type−SPT/DPT Reactions at the TET State during MD−FEP Simulations[a] (in Å)

	SPT	DPT
O(scissile peptide)−N(Ser195)	2.683 ± 0.064	2.680 ± 0.065
O(scissile peptide)−HN(Ser195)	1.729 ± 0.079	1.734 ± 0.077
O(scissile peptide)−N(Gly193)	3.034 ± 0.057	3.047 ± 0.063
O(scissile peptide)−HN(Gly193)	2.067 ± 0.080	2.077 ± 0.083
O_γ(Ser214)−$O_{\delta 1}$(Asp102)	2.570 ± 0.083	2.703 ± 0.095
H_γ(Ser214)−$O_{\delta 1}$(Asp102)	1.590 ± 0.096	1.752 ± 0.108
O(carbonyl,Ser214)−C_ϵ(His57)	3.065 ± 0.144	3.269 ± 0.163
O(carbonyl,Ser214)−H_ϵ(His57)	2.822 ± 0.151	3.155 ± 0.169
bending angle	92.81 ± 4.23	86.53 ± 3.34
O(carbonyl,Val213)−C $_\epsilon$(His57)	3.529 ± 0.146	3.625 ± 0.149
O(carbonyl,Val213)−H $_\epsilon$(His57)	2.488 ± 0.150	2.560 ± 0.149
bending angle	165.73 ± 3.52	174.46 ± 2.61

[a] These values are based on the additional 75 ps MD−FEP simulations at the TET state.

hole are similar in both the cases, the structures between His57 and Val213−Ser214 show slight difference. These conformational fluctuations bring a loss of the strong electrostatic stabilization in the TET state in the DPT reaction.

Although many experiments strongly supported the SPT mechanism rather than the DPT one, the exact position of the proton in the catalytic transition state has not been established. Proton inventory measurements suggested the DPT reaction mechanism for oligopeptides resembling naturally occurring substrates and pointed out the importance of the remote site interaction between the enzyme and substrates at the transition state, which is required to bring into action the fully developed catalytic potential.[9,10] The substrate used in this work is composed of six residues, which seems to be not so small compared with substrates used in many kinetic experiments. However, the present results strongly favor the SPT mechanism. The increase of the DPT activation free energy is mainly due to a loss of the stabilization effect around the active site, and these results are closely related to the structural changes between the triad and Val213−Ser214. To examine the importance of the remote site interaction, we performed additional MD−FEP simulations with extra harmonic constrain potentials, that bind the triad to Val213−Ser214. Based on the SPT reaction profile of the wild-type, we added the following three harmonic potentials at the catalytic transition state: $k_b = 500.0$ kcal/mol·Å^{-2}, $l_0 = 2.570$ Å, for O_γ(Ser214)−$O_{\delta 1}$(Asp102); $k_b = 100.0$, $l_0 = 3.520$, for O(carbonyl, Val213)−C_ϵ(His57); $k_b = 100.0$, $l_0 = 2.785$, for O(carbonyl, Ser214)−C_ϵ(His57). The resultant activation barrier increased by ∼4 kcal/mol from the SPT one but was still lower by ∼1 kcal/mol than that of the DPT. This result may indicate that if a specially designed substrate could bind two domains whose configuration is favorable to stabilize the catalytic transition state, DPT motion may be observed. However, for naturally occurring substrates, the DPT reaction seems less likely to proceed than the SPT one.

4. Conclusion

We have analyzed the role of Asp102 in the catalytic relay system of serine proteases based on the free energy profiles of the Ans102 mutant trypsin and the double proton-transfer reaction of the wild-type trypsin. In summary, Asp102 plays two important catalytic roles during the acylation. One is the strong electrostatic effect which stabilizes the protonated His57 formed along the catalytic pathway. This direct interaction apparently affects the electronic character of His57 as a base. The other is to fix the configuration around the active site, which is favorable to provide the catalytic environment. Also the protein environment around the active site is designed to stabilize the ionic state (Asp^- His^+ $oxyanion^-$) in the tetrahedral intermediate structure formed along the catalytic pathway. This environment prevents the proton transfer from His57 to Asp102, which is known as the charge-relay mechanism. The analyses of the remote site interaction between the enzyme and substrates during the catalytic process revealed that the interaction between His57 and Val213−Ser214 seems to be critical for the efficient hydrolysis of substrates.

Recently, the LBHB hypothesis has received much attention to rationalize the reaction mechanism of serine proteases.[13−15] Because the LBHB hypothesis is mainly supported by NMR measurements,[15] it will be worthwhile to carry out theoretical calculations of NMR chemical shifts for enzyme systems as in the present work.[32]

Acknowledgment. The author (T.I.) is grateful to Dr. Akihiro Morita for his valuable comments and continuous encouragement. The numerical calculations were carried out on the Computer Center of the Institute for Molecular Science (IMS). This work was supported by the Grant-in-Aid for Scientific Research from the Ministry of Education in Japan.

JA030405U

(32) Westler, W. M.; Weinhold, F.; Markley, J. L. *J. Am. Chem. Soc.* **2002**, *124*, 14373−14381.